

Received 17 May 2023, accepted 8 June 2023, date of publication 19 June 2023, date of current version 24 July 2023.

Digital Object Identifier 10.1109/ACCESS.2023.3287559



RESEARCH ARTICLE

Contrast Enhancement in Images by Homomorphic Filtering and Cluster-Chaotic Optimization

ÁNGEL CHAVARÍN^{ID}, ERIK CUEVAS^{ID}, OMAR AVALOS^{ID}, JORGE GÁLVEZ,
AND MARCO PÉREZ-CISNEROS

Departamento de Electrónica, CUCEI, Universidad de Guadalajara, Guadalajara, Jalisco 44100, Mexico

Corresponding author: Erik Cuevas (erik.cuevas@cucei.udg.mx)

This work was supported in part by Conacyt.

ABSTRACT Homomorphic filtering (HF) is a methodology that separates an image into two components: illumination and reflectance. Through the processing of these components, it is possible to significantly improve the contrast of the low-frequency components while preserving the edges and sharp features of the image. The parameter values of the filter that produces the best possible contrast enhancement depends on the image conditions for each image. However, finding the optimal parameters for the filter can be challenging, often involves a trial-and-error process, and can be prone to errors due to human factors. In this paper, we consider the problem of identifying the filter parameters as an optimization problem. Under such conditions, the cluster chaotic optimization (CCO) method is used to efficiently explore the parameter space by evaluating an objective function that assesses the contrast quality of an enhanced image. The experimental results show that the proposed method produces competitive results in terms of quality, stability, and accuracy compared with other methods on various datasets. Different metrics were evaluated to demonstrate the quality of the results of our method compared with the other algorithms.

INDEX TERMS Homomorphic filtering, metaheuristic algorithms, contrast enhancement, optimization algorithm, infrared images, color images.

I. INTRODUCTION

Image processing is an area of computer vision that has recently experienced exponential growth owing to the rise in mobile technology and continuous hardware improvements. One important area of image processing is image enhancement which refers to a set of techniques that aims to improve the visual quality of an image. Examples include Laplacian sharpening [1], [2], image averaging [4], image filtering [5], [6], and contrast enhancement [5], [7], [8], [9], [10], [11], [12].

Contrast enhancement is one of the most common image-enhancement techniques. Using these methods, the pixel intensity values are modified to produce high-quality images from a human perspective [9]. Several contrast enhancement

The associate editor coordinating the review of this manuscript and approving it for publication was Li He^{ID}.

techniques have been proposed in the literature. Some of the most common methods involve histogram equalization (HE) [12], contrast limited adaptive histogram equalization (CLAHE) [10], and average histogram equalization (AVHEQ) [4], to name a few. Despite acceptable results, they have two main flaws. For the first time, they distorted the resulting images by adding noise. Second, these methods cannot be used in combination with additional filters because the produced images present a loss of information. Contrast enhancement has several applications in various fields. The most important applications include underwater imaging [13], [14], medical imaging [15], and remote sensing [16].

On the other hand, there are other approaches, such as the top-hat transform [17], [18], and homomorphic filtering [5], [6], [19], [20], [21], that have been used as alternative techniques for contrast enhancement purposes. Homomorphic filtering (HF) is based on the superposition principle of

signals, which states that the sum of two or more signals can be obtained by adding their individual frequency components. HF separates an image into its illumination and reflectance components by applying a frequency-domain filter based on the logarithm of the image. Logarithmic transformation converts the multiplication of the illumination and reflectance components into an additive process. The filtering process is performed in the frequency domain, where the frequency components of the image are modified independently. After filtering, the components are combined using an inverse logarithmic transformation, which results in an enhanced image. The combination of HF with the difference of Gaussian (DoG) filters [22], [23] represents one of the best approaches that involve HF. Under this combination, several masks that consider different DoG filters are superimposed on the original image to remove noise and improve image quality. The performance of the combination of HF and DoG filters is directly related to the value of their parameters. Determining the optimal value for such parameters in a particular application is a difficult task that requires hundreds of tests, where the values are modified through experimentation.

Metaheuristic algorithms are programming techniques that emulate a heuristic (i.e., a learning strategy) to solve a set of generic optimization problems [24], [25], [26]. As no metaheuristic technique can solve all problems competitively, different approaches have been developed. Some examples include methods such as bio-inspired algorithms, which include genetic algorithms [9], swarm algorithms [8], [27], sociological algorithms [28], and ethnological algorithms [29], [30], [31], [32].

Metaheuristic methods have been recently utilized in the field of image processing, particularly for contrast enhancement of images. These methods have shown promising results in improving the quality of images with low contrast, making them more visually appealing and easier to interpret. One of the key advantages of using metaheuristic methods for contrast enhancement is their ability to handle complex and non-linear relationships between image pixels. Unlike traditional image processing techniques that often rely on simple mathematical models, metaheuristic methods can explore and exploit complex search spaces to find optimal solutions for contrast enhancement. Some examples of these approaches include the Genetic Algorithm (GA) described by in [9] and the artificial bee colony (ABC) algorithm described in [10].

Cluster-chaotic optimization (CCO) [38] method is a metaheuristic optimization algorithm that combines the principles of clustering and chaos theory to efficiently search for the optimal solution in a complex search space. The main advantage of the cluster-chaotic optimization method is its high convergence rate. The algorithm uses chaotic sequences to effectively explore the search space and avoid getting stuck in local optima, which leads to faster convergence to the global optimum. This is particularly advantageous for complex optimization problems with a large search space, where other optimization methods may require a long computation time to find the optimal solution.

This paper introduces a new image contrast enhancement technique based on homomorphic filtering (HF). In this study, the determination of the optimal parameters of a homomorphic filter is considered an optimization process in which the best values for the parameters that maximize the quality of the enhanced image are identified. In our approach, the CCO algorithm is used to detect the filter parameters that produce the best-enhanced images. Unlike other approaches, our method does not add distortions to the resulting image, thus providing better visual-quality results. The proposed approach is tested by considering different public datasets commonly used in the literature. The results were compared with those produced by other well-known enhancement techniques. The evaluation of the experimental results demonstrates that the proposed approach highlights the important details of the image, improving its visual appearance.

The remainder of this paper is organized as follows. In the second section, the main elements of homomorphic filtering and cluster-chaotic optimization are presented. The third section explains the proposed method. In the fourth section, the proposed method is compared with other existing schemes. Finally, in section five the conclusions of this study are discussed.

II. PRELIMINARY CONCEPTS

A. HOMOMORPHIC FILTERING

Homomorphic filtering [5] is a signal processing technique that is used to enhance images that are degraded by various factors such as noise, illumination, or contrast. The main idea behind homomorphic filtering is to divide an image $f(x, y)$ into its illumination $f_i(x, y)$ and reflectance $f_r(x, y)$ components. The illumination component refers to the amount and type of light that illuminates the scene or object, while the reflectance component refers to the inherent properties of the object or scene. The model that relates the image with its components can be formulated as follows:

$$f(x, y) = f_i(x, y) \cdot f_r(x, y) \quad (1)$$

The range of the illumination component is $0 < i(x, y) < \infty$ and reflectance component range is $0 < r(x, y) < 1$. Luminance is a low-frequency component, because the amount of illumination does not change significantly in this range. The reflectance component is a high-frequency component that changes significantly over this range [38]. The luminance and reflectance components are separated by applying the logarithmic transformation as follows:

$$\ln\{f(x, y)\} = \ln\{f_i(x, y) \cdot f_r(x, y)\} \quad (2)$$

Then, the Fourier transform is applied for processing images in the frequency domain:

$$F(u, v) = F_i(u, v) + F_r(u, v) \quad (3)$$

where $F_i(u, v) = FT\{\ln\{f_i(x, y)\}\}$ and $F_r(u, v) = FT\{\ln\{f_r(x, y)\}\}$. The filtered output $S(u, v)$ in the

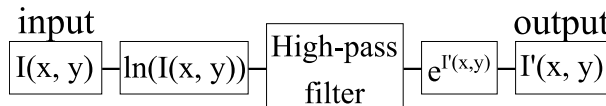


FIGURE 1. Representation of the homomorphic filtering.

frequency domain is modeled as follows:

$$S(u, v) = H(u, v) F_i(u, v) + H(u, v) F_r(u, v) \quad (4)$$

where $H(u, v)$ is a high-pass filter in frequency domain. The operation of $H(u, v)$ over the illumination F_i and reflectance F_r components allows obtaining an image $S(u, v)$ with enhanced contrast while preserving the overall shape and structure of the objects in the image.

After filtering, the inverse Fourier transform is applied to get a spatial domain image:

$$s(x, y) = IFT\{H(u, v) F_i(u, v)\} + IFT\{H(u, v) F_r(u, v)\} \quad (5)$$

Finally, the exponential function is applied to reconstruct the enhanced image as it is expressed in Equation (6)

$$g(x, y) = e^{\{s(x, y)\} = \ln\{g_i(u, v)\} + \ln\{g_r(u, v)\}} \quad (6)$$

The complete process conducted by the homomorphic filtering is illustrated in Figure 1.

B. DIFFERENCE OF GAUSSIANS

In our study, we use as high-pass filter $H(u, v)$ a Difference of Gaussians (DoG) filter. The DoG filter is particularly useful for enhancing edges and other sharp transitions in an image, as these features are often associated with high-frequency information. The DoG filter is modeled by the following expressions:

$$G(x, y) = \frac{1}{\sqrt{2\pi}} \left(e^{(-\alpha)} - e^{(-\beta)} \right) \quad (7)$$

where:

$$\alpha = \frac{(x+y)^2}{2\sigma_1^2}, \beta = \frac{(x+y)^2}{2\sigma_2^2} \quad (8)$$

where σ_1 and σ_2 corresponds to the parameters that define the effect of the filter. Determining the correct parameters of σ_1 and σ_2 often involves a trial-and-error process, where different parameter values are tested until the desired output is achieved.

C. THE CLUSTER-CHAOTIC-OPTIMIZATION (CCO)

The Cluster-Chaotic-Optimization (CCO) algorithm combines clustering and chaotic sequences to effectively explore the search space and avoid getting stuck in local optima. The clustering operation helps to maintain diversity in the population, while the chaotic sequences help to explore the search space in a random and efficient manner. CCO has been shown to be effective in finding the optimal values in several applications. CCO is a metaheuristic optimization method

used for finding the optimal values of a generic optimization problem formulated as follows:

$$\begin{aligned} &\text{Minimize/maximize } J(\mathbf{x}) \quad \mathbf{x} = (x_1, \dots, x_n) \in R^n \\ &\text{Subject to } \mathbf{x} \in \mathbf{S} \end{aligned} \quad (9)$$

where $J : \mathbf{R}^n \rightarrow \mathbf{R}$ is a nonlinear function and $\mathbf{S} = \{\mathbf{x} \in \mathbf{R}^n | l_j \leq x_j \leq u_j, j = 1, \dots, n\}$ is a bounded feasible space, constrained by the lower (l_j) and upper (u_j) limits. To solve the problem formulated in Eq. (9), CCO utilizes a population $D_k \left(\{d_1^k, d_2^k, \dots, d_{N_D}^k\} \right)$ of N_D candidate Solutions that evolve from the initial point ($k = 0$) to a total of gen number iterations ($k = \text{gen}$). Each individual $d_i^k \in [1, 2, \dots, N_D]$ represents an n -dimensional vector $\{d_{i,1}^k, d_{i,2}^k, \dots, d_{i,n}^k\}$ where each dimension corresponds to a decision variable of the optimization problem to be solved. After randomly initializing the population D_k in the search space, the set of individuals is processed considering three operations: clustering, intra-cluster, and extra-cluster. The iterative application of such procedures is executed until the number of generations has been reached. The perturbation α applied in intra-cluster and extra-cluster processes vary dynamically according to the following model:

$$\alpha = \lambda * \frac{s}{\eta} \quad (10)$$

where:

$$\lambda = \sum_{j=1}^n (u_j - l_j)^2 \text{ and } \eta = 100 * \text{gen} \quad (11)$$

The value of λ considers the sum of the differences among each dimension and 100 is a scale factor to normalize the perturbation α . The Algorithm 1 shows the complete operation of the CCO algorithm in form of pseudocode.

III. PROPOSED METHOD

Homomorphic filtering is an image processing technique that allow to separate the illumination and reflectance components of an image. The main advantage of homomorphic filtering over linear filtering is its ability to enhance the low-frequency components of an image while suppressing the high-frequency components, without affecting the edges or sharp features of the image. The parameters of the homomorphic filter affect the enhancement quality of the output image. Finding the optimal values for these parameters can be difficult because they depend on various factors such as the illumination conditions and the noise level. Determining the correct parameters for a homomorphic filter often involves a trial-and-error process, where different parameter values are tested until the desired output is achieved. This can be time-consuming and requires a good understanding of the underlying principles of homomorphic filtering.

In the proposed approach, the problem of finding the appropriate parameters of a homomorphic filter to enhance the contrast of images is considered an optimization problem. From an optimization point of view, this problem

is considered complex because of its discontinuity, high multimodality, and nonlinearity. In our scheme, the CCO metaheuristic method is used to identify the optimal parameters from the homomorphic filter. Because our approach considers the contrast enhancement problem, an appropriate objective function that effectively evaluates the quality of the enhanced images has also been proposed. In the proposed approach, it is identified the parameters of the HF filter through the CCO technique. The elements of the HF to be determined are σ_1 , and σ_2 . Under the CCO methodology, firstly, a set of n configurations (solutions) $\{\mathbf{x}_1, \mathbf{x}_2, \dots, \mathbf{x}_n\}$ is randomly initialized within the valid range of each parameter. Each solution \mathbf{x}_i consist of a vector of decision variables that includes both filter parameters σ_1^i and σ_2^i . Then, the image $I(x, y)$ is processed with the HF filter considering the parameters defined by \mathbf{x}_i . The resulting image $IEC(x, y)$ of the operation is evaluated by an objective function $J(IEC)$ to assess the quality of the solution \mathbf{x}_i in terms of enhanced contrast. Guided by the values of the objective function, the candidate solutions $\{\mathbf{x}_1, \mathbf{x}_2, \dots, \mathbf{x}_n\}$ are modified using the CCO operators so that they produce iteratively better solutions. This process is repeated until a determined criterion has been reached (a determined number of iterations). Finally, the optimal value of σ_1^i and σ_2^i corresponds to the configuration that delivers the image with the best possible enhanced contrast.

Figure 2 depicts the complete process of our contrast enhancement method. Firstly, the original image $I(x, y)$ undergoes a logarithmic transformation. Then, the Fourier transform is utilized to obtain $I(u, v)$, the logarithmic representation of the image in the frequency domain. Next, a Difference of Gaussians (DoG) filter $H(u, v)$ is applied to the image $I(u, v)$. The parameters σ_1^i and σ_2^i of the $H(u, v)$

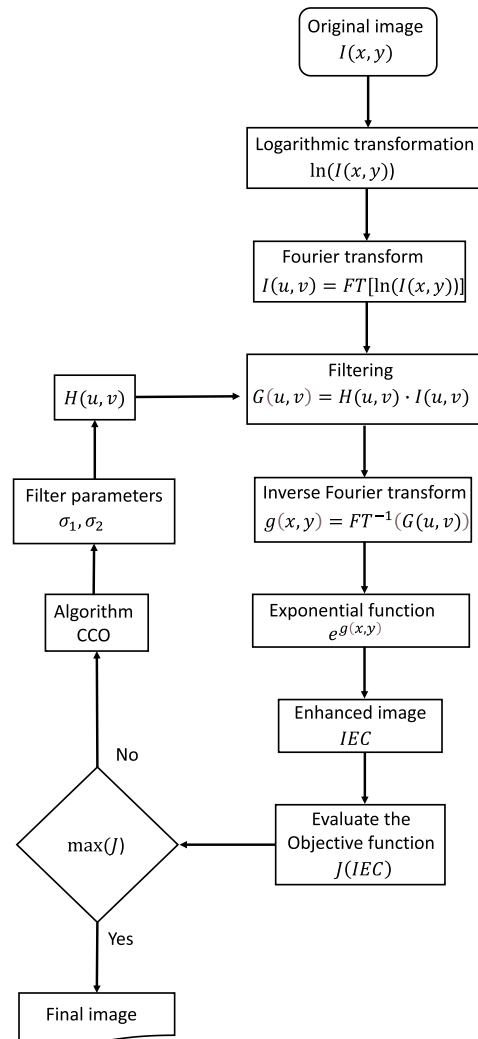


FIGURE 2. Complete process of our contrast enhancement method.

Algorithm 1 Pseudocode of the CCO

1. **Input** N_D , gen , $k=0$
2. $D^k \leftarrow initialize(N_D)$
3. **while** $k <= gen$ **do**
4. $d_B^k \leftarrow Select\ best\ particle(D^k)$
5. $[C_q^k, g] \leftarrow Clustering(D^k)$
6. $\alpha \leftarrow Calculate\ Perturbation(gen)$
7. **for** $(l=1; l <= g; q++)$
8. $d_b^k \leftarrow best\ Element\ Cluster(C_q^k)$
9. $d_l^{k+1} \leftarrow Local\ attraction(C_q^k)$
10. $d_l^{k+1} \leftarrow Local\ perturbation(d_l^{k+1})$
11. **end for**
12. **for** (all best cluster elements of C_q^k)
13. $d_b^{k+1} \leftarrow Global\ attraction(d_b^k)$
14. $d_b^{k+1} \leftarrow Global\ perturbation(d_b^{k+1})$
15. **end for**
16. $k=k+1$
17. **end while**
18. **Output:** d_B^k

filter is continuously updated by the CCO algorithm. Subsequently, the filtered image $G(u, v)$ is transformed back to the space domain using the Inverse Fourier transform. The final enhanced image IEC is generated by applying an exponential transformation to the filtered image $g(x, y)$. To evaluate the quality of IEC , an objective function J is employed. If the quality of IEC is not optimal, the CCO algorithm explores the parameter space to find another set of parameters σ_1^i and σ_2^i . The filtering process is repeated until the best possible enhanced image is obtained. The CCO algorithm allows to optimize the filter parameters to obtain the best possible image enhancement. Overall, this process is iterative and involves modifying filter parameters until the desired level of contrast enhancement is achieved. The best enhanced image IEC obtained from this process is considered the final output. Our method has been designed to provide the best possible contrast enhancement while maximizing the quality of IEC .

A. OBJECTIVE FUNCTIO

Defining an appropriate objective function is crucial for evaluating the quality of the enhanced image $IEC(x, y)$ because it

provides a way to assess the perceptual qualities of the image, such as brightness, contrast, and sharpness. By defining an appropriate objective function, the optimization algorithm can be effectively guided to determine the optimal solution that represents the best contrast of the image while maintaining its perceptual qualities. In this study, the objective function used to evaluate the quality of the enhanced image *IEC* in terms of enhanced contrast is described as follows:

$$J(IEC) = \log(\log(E(IEC))) \cdot \frac{ne(IEC)}{M \cdot N} \cdot H(IEC) \quad (12)$$

where:

- $J(IEC)$ Represents the quality of the enhanced image *IEC* obtained as a candidate solution of the optimization process.
- $E(IEC)$ is the sum of edge intensities of the image resulting from filtering the image *IEC* by the Sobel filter.
- $ne(IEC)$ is the number of edges obtained in $E(IEC)$.
- $H(IEC)$ is the entropy of *IEC*.
- M and N are the dimensions of the image.

The objective function $J(IEC)$ evaluates the quality of the contrast of the image *IEC* based on three elements: sum of edge intensities $E(IEC)$, number of edges $ne(IEC)$, and entropy $H(IEC)$. The sum of the edge intensities, obtained by filtering the image with the Sobel filter, measures the total amount of high-frequency information in the image. This high-frequency information represents the edges and details of the image, which are important for visual perception and contrast. The number of edges obtained also provides information about contrast quality. A higher number of edges indicates a better distinction between regions with different intensities. Finally, entropy provides an indirect evaluation of contrast through intensity values. An image with high entropy (better contrast) had a wide range of intensity values, whereas an image with low entropy (worse contrast) had fewer intensity values. High entropy is generally desirable in images, as it indicates a higher level of detail and texture, which contribute to the image contrast.

This objective function has been already used to evaluate the quality of images for other proposed such as segmentation [36], classification [37], etc. Algorithm 2 outlines all the steps involved in the proposed scheme, which integrates Homomorphic filtering and the optimization CCO technique. The algorithm begins by applying a Homomorphic filter. This filter enhances the image by reducing the effect of low-frequency noise, making it easier to process. Next, the optimization CCO technique is. This technique involves maximizing an objective function that evaluates the quality of the enhanced image.

IV. EXPERIMENTAL RESULTS

In this section, the experimental section is discussed. The aim of this section is to evaluate the performance of the proposed approach in comparison to other similar methods, by conducting a set of complex tests. The tests have been designed to assess the quality, stability, and accuracy of the

Algorithm 2 ICE-CCO Pseudocode

Input image I

Convert image to double values

Run metaheuristic algorithm (*CCO*):

Input $N_D, gen, k = 0$

$D_B^K \leftarrow Initialize(N_D);$

While $k <= gen$ **do**

$D_B^k \leftarrow SelectBestParticle(D_B^k);$

$[C_q^k, g] \leftarrow clustering(D_B^k);$

$\alpha \leftarrow CalculatePerturbation(gen);$

For $(q = 1; q <= g; q++)$

$d_b^k \leftarrow BestElementCluster(C_q^k);$

$d_l^{k+1} = LocalAttraction(C_q^k); l \in C_q^k$

$d_l^{k+1} = LocalPerturbation(d_l^{k+1});$

End for

For (all best cluster elements of C_q^k)

$d_b^{k+1} \leftarrow GlobalAttraction(d_b^k);$

$d_b^{k+1} \leftarrow GlobalPerturbation(d_b^{k+1});$

End for

$k=k+1;$

end while

Output: d_B^k (2 dimensions)

Assign σ_1, σ_2 values from d_B^k

Convert to logarithm scale to separate luminance and reflectance

FFT($L(x, y) + R(x, y)$)

Difference of gaussians filter(h)

Convert to high frequency filter ($H = I - h$)

IFFT($Z(x, y)$)

Convert to exponential scale (logarithmic-exponential cancellation principle)

Output Image

output images obtained using the proposed approach, as well as to compare its performance against other state-of-the-art methods for contrast enhancement. Various datasets are used to test the proposed approach, including images with different illumination conditions, noise levels, and contrast ranges.

A set of representative images extracted from different public datasets [45], [46] has been used to evaluate the performance of the proposed approach. Such datasets include several low-contrast images with different levels of complexity. The set of experiments has been tested on equipment with the following characteristics: Ryzen 5 1600 processor, 3.2 GHz 6-core, 20Gb DDR4 RAM, 2400MHz, GeForce GTX 1650 Graphic card 4Gb DDR5, Solid state disk baracuda WD 240 Gb, Matlab 2019a.

This section consists of four parts. The first part presents the evaluation criteria for the general experimentation. The second part consists of experiments with other enhancement methods such as Hashemi and Draa. The third part involves experimentation with enhancement techniques, such

as CLAHE or MSA-ICE, in grayscale images. Finally, the fourth section presents the experimental results of the color images.

A. PERFORMANCE INDEXES FOR THE EXPERIMENTS

To evaluate the quality of the results, six different performance indexes have been used: Mean squared error (*MSE*), Structural similarity index measurement (*SSIM*), Edge Preserve Index (*EPI*), Entropy (*E*), Relative Enhancement Contrast (*REC*), Range Redistribution (*RR*) and, in the case of the color images, colorfulness (*C*). In addition, the metric peak-to-noise ratio (*PSNR*) is also considered.

The first six indices are chosen for the comparisons to maintain compatibility with other similar ICE methods. The seventh metric (colorfulness) is used to compare the modification of the colors in the image. To determine its value, each quality index considered the original image **R** with poor contrast values. This image is considered as the input in the Image Contrast Enhancement (ICE) method. Consequently, an enhanced image **I** is generated.

MSE evaluates the similarity between the enhanced image **I** and its reference **R** by subtracting the pixel values of the enhanced image from the pixels of its reference and then calculating the mean value of the total error [42]. The *MSE* is obtained using the following model:

$$MSE = \frac{1}{MN} \sum_{i=1}^M \sum_{j=1}^N (I(i,j) - R(i,j))^2 \quad (13)$$

The Structural similarity index measurement (*SSIM*) evaluates the similarity between the improved image **I** and the original **R**. Assuming that $\{p_1, \dots, p_{M \times N}\}$ represents the pixels from **I** and $\{r_1, \dots, r_{M \times N}\}$ the original pixels from **R**, the *SSIM* [44] is computed as follows:

$$SSIM = \frac{(2\mu_I\mu_R + Q_1)(2\sigma_{IR} + Q_2)}{(\mu_I^2 + \mu_R^2 + Q_1)(\mu_I^2 + \mu_R^2 + Q_2)} \quad (14)$$

where Q_1 and Q_2 symbolize two small positive constants (typically 0.01). μ_I and μ_R correspond to the mean values of the enhanced and reference data, respectively. σ_I and σ_R represent the variance of the enhanced and reference data, respectively. σ_{IR} is the covariance of both data elements **I** and **R**.

The edge preservation index (*EPI*) evaluates the edge preservation of the produced image **I** with respect to the original image **R** [45]. The higher the *EPI* value, the better the performance of the algorithm. It is calculated according to the following expression:

EPI

$$= \frac{\sum_{i=1}^M \sum_{j=1}^N |I(i,j) - I(i,j+1)| + |I(i,j) - I(i+1,j)|}{\sum_{i=1}^M \sum_{j=1}^N |R(i,j) - R(i,j+1)| + |R(i,j) - R(i+1,j)|} \quad (15)$$

Entropy (*E*) evaluates the information content of the image [35]. It is a measure of quality that indirectly considers

the number of details in the enhanced image; therefore, the higher the value, the better the results obtained.

$$E = - \sum_{i=0}^{L-1} P(q) \cdot (\log(P(q))) \quad (16)$$

where $P(q)$ is the probability density function at intensity level q ($q \in 0, \dots, L - 1$) of an image **I**. L symbolizes the total number of grayscale levels contained in the image **I**.

The range redistribution (*RR*) [47] indicates how the pixel intensities are distributed in the enhanced image regarding the original image [44]. Its value is computed as follows:

$$RR = \frac{1}{M \times N \cdot (M \times N - 1)} \sum_{q=1}^{L-1} \sum_{r=q}^{L-1} P(q) P(r) (r - q) \quad (17)$$

where $P(q)$ and $P(r)$ represent the probability density function at levels q and r , respectively, ($q, r \in 0, \dots, L - 1$) of the enhanced image. L is the total number of gray levels existing in the image. A high value of this index means that the histogram is better distributed without pixel concentrations.

Relative contrast enhancement (*REC*) [49] is a metric that quantifies the contrast between an enhanced image **I** and the original image **R**. A higher value will mean better performance. Its formulation is given by:

$$REC = 20 * \log \left[\frac{1}{M \times N} \sum_{i=1}^M \sum_{j=1}^N (I(i,j))^2 - \left(\frac{1}{M \times N} \sum_{i=1}^M \sum_{j=1}^N R(i,j) \right)^2 \right] \quad (18)$$

The *PSNR* measures the quality between the original and the enhanced image [43]. The higher the *PSNR*, the better the image quality of the enhanced image. The *PSNR* value is computed as follows:

$$PSNR = 10 \log_{10} \left(\frac{F^2}{RMSE} \right) \quad (19)$$

where F is the maximum fluctuation of the input image.

The Visual Information Fidelity (*VIF*) index [13] is a measure of the similarity between two images that takes into account the properties of the human visual system. It is calculated using a combination of spatial and frequency domain analysis. Its computation requires a complete procedure [13] that can be summarized in the following equations.

$$VIF = \mu_s^2 \cdot \sigma_l \cdot \sigma_h \cdot \rho \quad (20)$$

where μ_s is the mean squared difference between the images **I** and **R** in the spatial domain, σ_l and σ_h are the standard deviations of the differences between the images **I** and **R** in the low and high frequency regions, respectively, and ρ is the cross-correlation coefficient between the images **I** and **R** in the frequency domain. A high value of *VIF* means a better visual quality in the image.

In addition to the aforementioned indices, the Colorfulness (C) index is also incorporated. The Colorfulness (C) index [50] indicates the amount of color in an image based on a visual standpoint. A larger C value implies better color perception. The calculation of C involves the three-color channels, R , G , and B , in an I_{RGB} image, and can be expressed as follows:

$$C = \sigma_{RGYB} + (0.3 \times \mu_{RGYB}) \quad (21)$$

where:

$$\sigma_{RGYB} = \sqrt{\sigma_{RG}^2 + \sigma_{YB}^2} \quad \mu_{RGYB} = \sqrt{\mu_{RG}^2 + \mu_{YB}^2} \quad (22)$$

The evaluation of color perception using this metric depends on the mean μ and standard deviation σ of all the pixels present in the channel differences RG and YB . These channel differences are defined as follows:

$$G = (R - G) \quad YB = 0.5 \times (R + G) - B \quad (23)$$

B. COMPARISON WITH POPULAR METAHEURISTIC METHODS

The objective of this subsection is to compare the results of the proposed method (called ICE-CCO) with popular contrast enhancement methods that consider metaheuristic principles in their operation. These methods represent techniques that are widely used and referenced in the literature. The results of this experiment are presented in Table 1, which shows the performance of various contrast enhancement methods on images with poor contrast. These results have been obtained by using popular algorithms such as the genetic algorithm (GA) described by Hashemi [9] and the artificial bee colony (ABC) algorithm described by Draa [10]. The objective was to compare the effectiveness of these methods in enhancing the contrast of images that lack of sufficient contrast. The study utilized images from the messier catalog [47] to evaluate the performance of the contrast enhancement methods. The Messier catalog contains a collection of astronomical objects that are often used as a benchmark dataset for evaluating image processing algorithms. The images from this catalog were selected because they present a significant challenge for contrast enhancement due to their poor contrast.

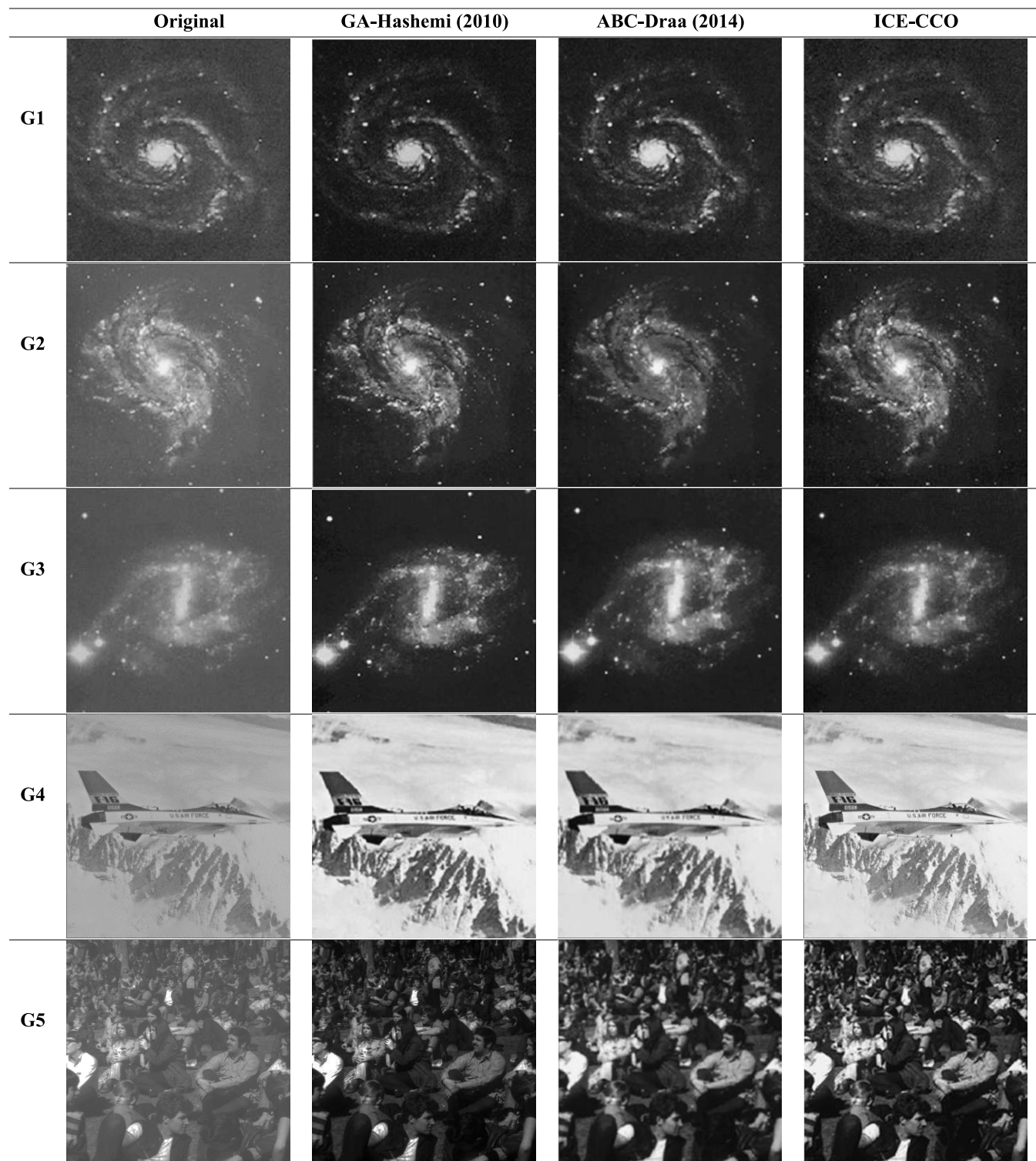
All the algorithms used in the analysis were set using the parameters suggested by their respective references. This was done to ensure that the comparisons were fair and that each algorithm was evaluated based on its optimal performance. However, all methods consider a population $N = 25$ and $iterations = 50$, in their operation.

The results presented in Table 1 indicate that the proposed contrast enhancement method ICE-CCO is superior to the genetic algorithm (GA) and artificial bee colony (ABC) algorithm in terms of visual quality. The ICE-CCO method produces images that are clear and not oversmoothed, which is an essential characteristic in image processing. In comparison, GA and ABC methods have a tendency to remove edges and other significant elements, which results in less

aesthetically pleasing images. Although most methods produced similar outcomes for astronomical images (G1-G3), real-life images (G4-G5) displayed noticeable differences among the techniques. The ICE-CCO method proposed in this study, however, was capable of generating exceptional images without compromising the critical characteristics of the original images. The method emphasized the features in the images, leading to an improved visual perception of the images. The algorithm's ability to detect the global optimum, which corresponds to the best possible enhanced image, is one of its remarkable features. This ability is attributed to the metaheuristic CCO algorithm. It allows for the efficient identification of the optimal solution in a complex search space. In such conditions, this optimization technique is effective in enhancing image contrast, resulting in visually appealing images that highlight important image features while maintaining their natural appearance. This feature is crucial in various applications, including medical imaging, surveillance, and astronomy, where accurate image analysis is critical. When assessing image contrast improvement, there are numerous visual details to consider, with overall brightness being one critical aspect.

Table 1 indicates that the proposed ICE-CCO method generates images with a well-balanced overall brightness, meaning that the image is neither excessively dark nor excessively bright. This attribute is crucial since an overly dark or bright image can negatively impact its visualization and make it difficult to distinguish its features. Conversely, the GA and ABC methods create images that lack this balance, making it challenging to perceive the image's features. Texture is another essential aspect to evaluate in image enhancement. Texture refers to the visual patterns and variations present in the image, such as the surface roughness or fine details of a pattern. An examination of Table 1 reveals that the ICE-CCO method enhances the texture of several regions in the image, making it easier to discern its features. This capability can be particularly important in specific applications. In contrast, the GA and ABC methods tend to have a negative impact on the visualization of texture areas in the image. This is due to their tendency to over-smooth the image, which can eliminate the fine details and patterns. This drawback can make it challenging to appreciate the features of the image and affect the interpretation of the image. The ability of our approach to obtain images with well-balanced and distinguishable textures is a consequence of the entropy considered in the objective function. With the integration of entropy, an image with a wide range of intensity values is preferred to an image with fewer intensity values.

To expand the evaluation of the proposed approach, a new study was conducted. In this experiment, two different performance indexes, the PSNR [43] index and the number of edges, were used to test the quality of the results of the ICE-CCO approach. These indices are only used for this introductory analysis. Then, the complete set of performance indexes will be used in the following experiments.

TABLE 1. Visual results from GA, ABC and the proposed ICE-CCO method.

In image contrast enhancement, the PSNR index can be utilized as a quantitative metric to assess the quality of the processed image compared to the original image. A higher PSNR value denotes better image quality. Table 2 presents

a comparison of the results on the PSNR index. The results indicate that the ICE-CCO approach outperforms the GA and ABC techniques in terms of the PSNR values. This suggests that the proposed approach does not affect the structures and

TABLE 2. PSNR metric from GA, ABC and the proposed method (ICE-CCO).

Image	GA	ABC	ICE-CCO
G1	14.16	23.64	27.4711
G2	13.21	12.18	17.0105
G3	13.75	17.42	25.5680
G4	20.12	20.16	25.3994
G5	17.92	24.84	16.2187

TABLE 3. Comparison of Edges from GA, ABC and the proposed method (ICE-CCO).

	GA	ABC	ICE-CCO
G1	1.96E+03	1.33E+03	2.58E+03
G2	2.50E+03	2.90E+03	4.31E+03
G3	2.88E+03	2.17E+03	3.88E+03
G4	3.49E+03	3.53E+03	8.98E+03
G5	3.32E+03	2.56E+03	9.16E+03

characteristics of the image, which helps to avoid deformations that could result in a loss of information. The results show that the ICE-CCO approach presents higher PSNR values in almost all images, except for image G5, where the ABC technique achieved a better solution in terms of the PSNR index. This could be due to the image's characteristics, which may have required a different approach to achieve optimal results. The high PSNR values obtained with the ICE-CCO approach can be attributed to the capabilities of the Homomorphic filter, which removes noise from images while improving contrast, resulting in sharper results that are easier to perceive by the human eye.

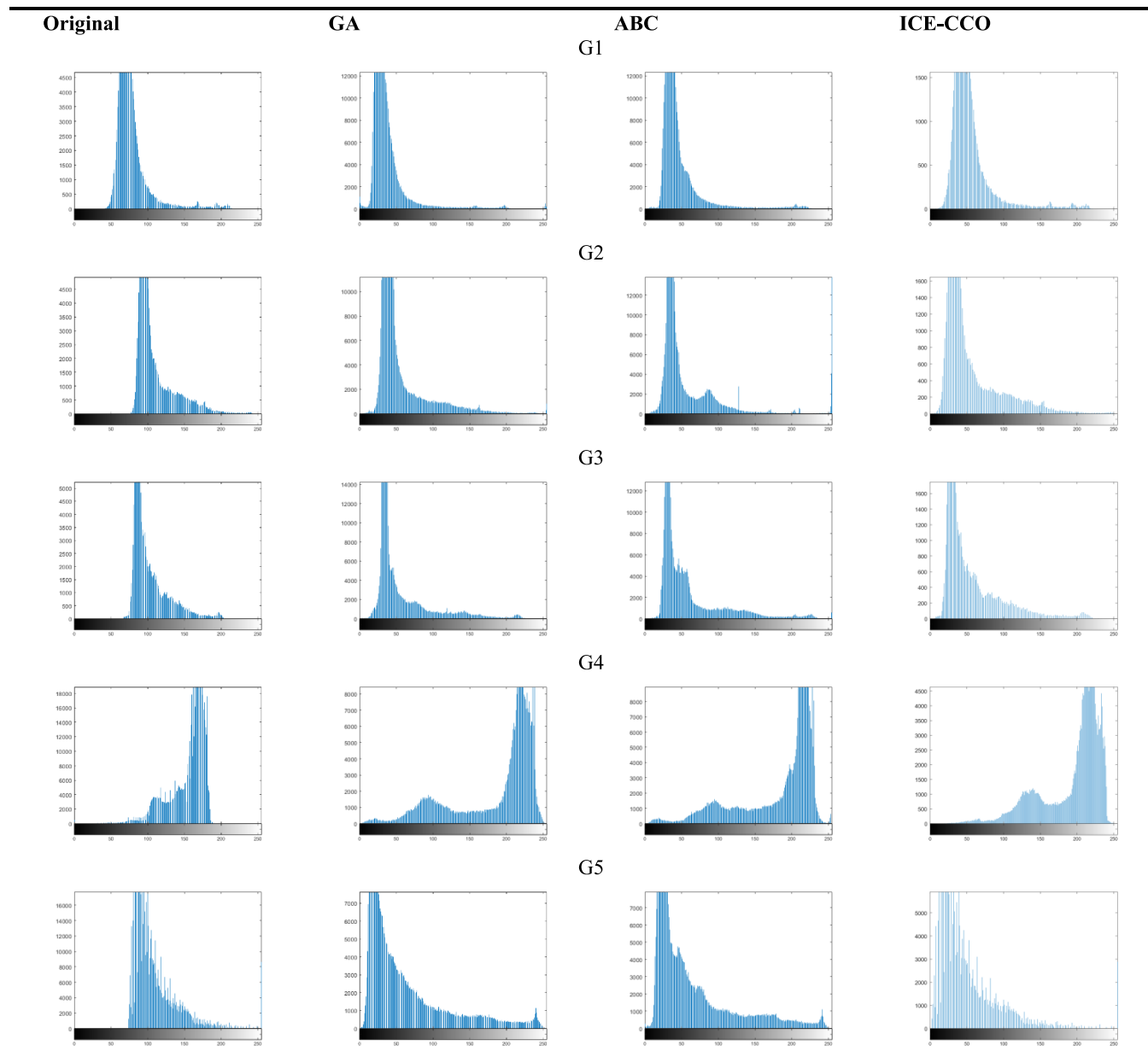
Table 3 provides a comparison of the number of edges obtained with the proposed ICE-CCO method, as well as with the GA and ABC techniques. The results show that the ICE-CCO method maintains the best values in terms of the number of edges, in comparison to the GA and ABC techniques. This means that the ICE-CCO method is able to preserve the edges of the image while enhancing the contrast, producing images with better visual quality. From Table 3, it is also clear that the GA method maintains the second place in terms of the number of edges, while the ABC method obtains the worst values. This suggests that the GA method is also able to preserve the edges of the image to some extent, although not as effectively as the ICE-CCO method. The ABC method, on the other hand, may have a tendency to smooth out the image and reduce the number of edges, resulting in a loss of important information and details. The number of edges in an image is a measure of the sharp transitions between different intensities in the image. These edges are important features of an image that can provide information about its content and structure. In contrast enhancement, preserving edges is particularly important as they can affect the visual quality of the processed image. Some methods may reduce the number of edges, resulting in a smoother image, while others may increase the number of edges, resulting in a sharper image with more pronounced transitions. The number of edges can be used to measure the quality of a contrast enhancement method. A good method

should preserve important edges while enhancing contrast. A reduction in the number of edges may result in a loss of important details, while an increase may create an image that looks unnatural. Comparing the number of edges in the processed image to the original image is important to determine if important edges have been preserved. If the number of edges in the processed image is higher, it may indicate that important edges have been preserved, while a significantly lower number of edges may indicate that important edges have been lost. The capacity to produce images with defined borders and noticeable objects or regions is a consequence of the employed objective function, which considers the sum of the edge intensities and the number of edges to select the best enhanced image. Therefore, an image with more edges and details would have a better probability of being identified than an image with blurred elements.

Histograms are a graphical representation of the frequency distribution of pixel intensities in an image. They provide useful information for analyzing contrast and brightness, as well as evaluating the quality of a contrast enhancement method. The shape of the histogram can reveal important details about the distribution of pixel intensities in the image and how a contrast enhancement method affects it. A good method should maintain the important details and features of the image while stretching or compressing the histogram to cover the full range of intensity values. If the histogram is compressed or stretched too much, it may indicate over- or under-enhancement, resulting in a loss of details or features. Similarly, if the histogram is shifted too much, it may indicate that the method has changed the brightness of the image too much, leading to an unnatural appearance. Table 4 displays the histograms generated by the different contrast enhancement techniques examined. According to Table 4, it can be observed that the ICE-CCO algorithm generates histograms that have a superior distribution of grayscale values when compared to the GA and ABC methods. The histogram created by the ICE-CCO approach exhibits a well-proportioned distribution of pixel intensities throughout the entire grayscale range, suggesting that it is effective in improving image contrast while retaining a natural and well-balanced overall brightness. A well-balanced overall brightness is critical since it facilitates the perception and differentiation of image features. Conversely, the histograms produced by GA and ABC are similar to the original histogram, indicating that their contrast enhancement is only marginal, making them less effective than ICE-CCO in enhancing image contrast. The histograms produced by GA and ABC also demonstrate that they are incapable of achieving a balanced overall brightness, which can have an adverse impact on image visualization.

C. EXPERIMENTS WITH STATE-OF-THE-ART TECHNIQUES

In this section, the proposed ICE-CCO contrast enhancement method is compared with other state-of-the-art techniques that have been published recently. These methods include the contrast limited adaptive histogram equalization (CLAHE)

TABLE 4. Histograms from historical algorithms and the proposed method.

and the moth swarm algorithm (MSA-ICE). To evaluate the performance of the different techniques, several performance indexes are used, as discussed in subsection IV-A. These performance indexes involve the Mean squared error (*MSE*), Structural similarity index measurement (*SSIM*), Edge Preserve Index (*EPI*), Entropy (*E*), Range Redistribution (*RR*), Relative Enhancement Contrast (*REC*) and Visual Information Fidelity (*VIF*). In the comparisons, it has been used six representative images ($I_1 - I_6$) extracted from several datasets. The images have different levels of distortions such as sharpness, brightness, overexposure, low contrast, etc. By using this group of images, the comparison results will be more realistic and reliable, allowing to analyze the

performance of each technique in a variety of scenarios. In order to ensure a fair comparison between the proposed ICE-CCO and the state-of-the-art approaches, the algorithms used in the experiments have been set using the parameter values suggested by their own references. The only different parameter of MSA-ICE is the number of sub-trial vectors nc . This parameter, according to its reference, depends on the application. For this reason, it has been set to $nc = 8$. As both MSA and ICE-CCO are methods based on metaheuristic principles, they have been also configured with $iter = 30$ and $population = 15$. This setting ensures that the algorithms have enough time to converge to a good solution while avoiding overfitting and reducing the computational cost.

By using the recommended parameter values, the comparison between the methods is not biased and allows for a fair evaluation of their performance.

Table 5 presents the results of the CLAHE, MSA-ICE, and the proposed ICE-CCO methods for image enhancement. A careful analysis of Table 5 shows that the best visual quality of the images is obtained by the proposed ICE-CCO method. In fact, all the enhanced images generated by the ICE-CCO method present a better balance between the dark and bright group of pixels, resulting in images that are visually more pleasing to the human eye. In contrast, the CLAHE and MSA-ICE algorithms produce dark images as they are unable to reach an appropriated contrast. The inability of these methods to obtain a balanced contrast is evident in Table 5. An analysis of Table 5 also demonstrates that the important characteristics of the image are highlighted in the case of the ICE-CCO method, while the CLAHE and MSA-ICE tend to eliminate such features. This makes the ICE-CCO method superior in highlighting the details such as edges or corners of the image. Furthermore, textures of the images are better processed in the case of the ICE-CCO approach, enhancing the fine details of the textures. The CLAHE and MSA-ICE tend to over smooth or darken the textures, which avoids a correct visualization of texture regions. This makes the ICE-CCO method superior in terms of texture processing and highlighting details.

Table 6 presents a comparison of the performance of three different image enhancement methods, namely CLAHE, MSA-ICE, and ICE-CCO. The evaluation is based on seven performance indexes, namely Mean squared error (*MSE*), Structural similarity index measurement (*SSIM*), Edge Preserve Index (*EPI*), Entropy (*E*), Range Redistribution (*RR*), Relative Enhancement Contrast (*REC*) and Visual Information Fidelity (*VIF*). The *MSE* measures the similarity between the enhanced image and its reference, while the *SSIM* measures the similarity between the improved image and the original. From Table 6, it is evident that the proposed ICE-CCO algorithm achieves better *MSE* and *SSIM* values than the other two methods. This means that the ICE-CCO produces images that are more similar to the reference and the original images, respectively, and therefore have less distortion. The *EPI* measures the preservation of edges in the enhanced image with respect to the original image. The ICE-CCO method outperforms the other two methods in terms of *EPI*, indicating that it better preserves the edges of the original image in the enhanced image. However, it is worth noting that the MSA-ICE also performs well in terms of *EPI*. The Entropy (*E*) index evaluates the information content of the image, and indirectly considers the number of details in the enhanced image. The ICE-CCO method produces images with higher entropy values than the other two methods, indicating that it enhances contrast while preserving important details in the image. The *RR* measures the redistribution of pixel intensities in the enhanced image. The ICE-CCO method outperforms the other two methods in terms of *RR*, indicating that it better distributes the pixel

intensities in the enhanced image. The *REC* measures the contrast enhancement between the enhanced image and the original image. The proposed ICE-CCO method achieves better *REC* values than the other two methods, indicating that it provides better contrast enhancement results. In summary, the proposed ICE-CCO algorithm outperforms the CLAHE and MSA-ICE methods in terms of *MSE*, *SSIM*, *EPI*, Entropy (*E*), *RR*, and *REC*. Finally, *VIF* is an index used to evaluate the visual quality of images by considering the properties of the human visual system. It is based on the fact that the human visual system is sensitive to certain types of distortions in images, and therefore the method takes into account the perceptual characteristics of the human eye. In the case of image contrast enhancement, *VIF* can be used to assess the visual quality of the processed image. The higher the *VIF* value, the better the visual quality of the image. This is because a higher *VIF* value indicates that the processed image contains more information that is perceptually relevant to a human observer. Table 6 reports the results of the *VIF* evaluation for the different contrast enhancement methods. The results show that the ICE-CCO method produces images with the best visual quality in terms of human perception, as it presents the highest values of *VIF*. The MSA-ICE method follows, presenting lower values than ICE-CCO. On the other hand, the CLAHE method produces images with the worst visual quality, presenting the lowest values of *VIF*. These results suggest that the proposed ICE-CCO method is able to generate images that are more visually appealing to a human observer than the other contrast enhancement methods. This is because the method is able to preserve important visual features of the image while enhancing its contrast, resulting in images that are visually more appealing and easier to interpret. Therefore, the ICE-CCO method can be considered a reliable and effective method for contrast enhancement of images, especially in applications where the visual quality of the image is of critical importance, such as in medical imaging or material science.

The comparison of the results indicates the effectiveness of the proposed approach in enhancing image contrast while preserving crucial details and edges. The histograms produced by each contrast enhancement technique are also displayed in Table 7. Upon examining the table, it can be concluded that the ICE-CCO algorithm provides a superior grayscale value distribution compared to the CLAHE and MSA-ICE methods. The ICE-CCO histogram demonstrates a well-proportioned distribution of pixel intensities throughout the entire grayscale range, indicating that the algorithm is highly successful in enhancing image contrast while maintaining a natural and well-balanced overall brightness. This balanced brightness is essential for easy visualization and identification of image features. In contrast, the histograms generated by CLAHE and MSA-ICE methods are similar to the original histogram, implying that their contrast enhancement is only minimally effective. Therefore, these techniques are less effective than ICE-CCO in enhancing image contrast. Furthermore, the

TABLE 5. Visual comparison between ICE-CCO, CLAHE and MSA-ICE.

ORIGINAL	CLAHE	MSA-ICE	ICE-CCO

histograms produced by CLAHE and MSA-ICE methods demonstrate their inability to balance the overall brightness

of the image, which can have an unfavorable impact on image visualization.

TABLE 6. Numerical comparison among CLAHE, MSA-ICE and ICE-CCO with grayscale images.

Image	Metric	CLAHE	MSA-ICE	ICE-CCO
I ₁	<i>SSIM</i>	0.7874	0.9121	0.9984
	<i>MSE</i>	7.26E+03	7.22E+03	0.0114
	<i>EPI</i>	1.0567	1.3412	0.9943
	<i>E</i>	5.9740	6.8714	7.5258
	<i>RR</i>	1.0010	1.2101	1.0672
	<i>REC</i>	38.7410	47.1240	80.8165
	<i>VIF</i>	1.1787	1.2841	1.4427
I ₂	<i>SSIM</i>	0.7011	0.7941	0.9984
	<i>MSE</i>	5.67E+03	4.71E+03	0.0116
	<i>EPI</i>	0.9642	1.0874	0.9959
	<i>E</i>	4.5787	5.8471	7.4388
	<i>RR</i>	0.9057	1.0074	1.0998
	<i>REC</i>	31.7421	39.7487	82.8337
	<i>VIF</i>	1.2060	1.2639	1.4835
I ₃	<i>SSIM</i>	0.5074	0.6072	0.9984
	<i>MSE</i>	3.98E+03	3.41E+03	0.0109
	<i>EPI</i>	0.9101	0.99814	0.9849
	<i>E</i>	3.9740	4.8721	6.1682
	<i>RR</i>	0.8714	0.9941	1.0122
	<i>REC</i>	35.7840	42.3180	56.2866
	<i>VIF</i>	1.4832	1.5241	1.6222
I ₄	<i>SSIM</i>	0.6024	0.6921	0.9992
	<i>MSE</i>	6.36E+03	6.21E+03	0.0058
	<i>EPI</i>	1.0009	1.2101	0.9982
	<i>E</i>	4.0874	5.1401	6.3181
	<i>RR</i>	0.9872	1.1921	1.1525
	<i>REC</i>	27.1024	35.8724	140.9974
	<i>VIF</i>	1.1394	1.2879	1.3378
I ₅	<i>SSIM</i>	0.9417	0.9714	0.9986
	<i>MSE</i>	8.01E+03	7.02E+03	0.0105
	<i>EPI</i>	0.9014	1.0254	0.9957
	<i>E</i>	5.8914	7.1101	7.1577
	<i>RR</i>	0.8874	1.0074	1.1058
	<i>REC</i>	31.0440	37.1421	97.0714
	<i>VIF</i>	1.2175	15614	1.6380
I ₆	<i>SSIM</i>	0.5514	0.6421	0.9985
	<i>MSE</i>	3.87E+03	3.10E+03	0.0103
	<i>EPI</i>	0.9821	1.1121	0.9992
	<i>E</i>	4.7784	5.2140	7.5409
	<i>RR</i>	0.9974	1.1987	1.1192
	<i>REC</i>	39.5870	45.1470	98.2521
	<i>VIF</i>	1.1953	1.3698	1.6539

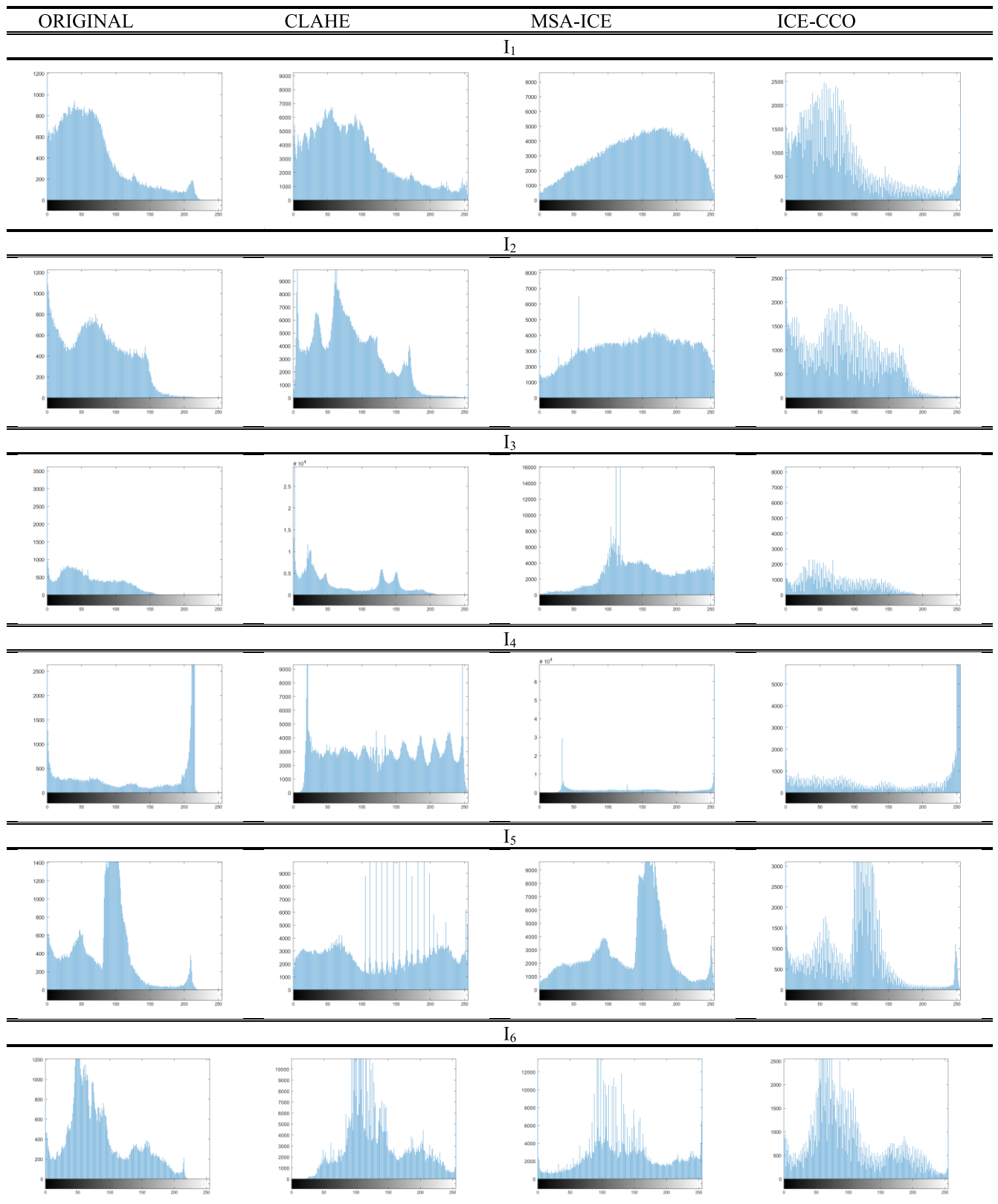
D. COMPARISON OF COLOR IMAGE

When a color image has better contrast, it means that the differences in brightness and color between different parts of the image are more apparent and visually distinct. In other words, the brighter and darker areas of the image are more clearly defined, and the colors in the image are more vivid and distinguishable. A color image with good contrast allows the viewer to easily distinguish and interpret the details and features of the image, making it more visually appealing

and informative. On the other hand, a color image with poor contrast may appear dull, flat, or washed out, and the details and features of the image may be difficult to distinguish. The contrast color enhancement method starts by taking an input color image $I_{RGB} = \{R, G, B\}$ in the RGB format. Then, this I_{RGB} image is converted into the HSI space using the transformation $I_{HSI} = T \{I_{RGB}\}$. Afterward, the intensity I -channel of the I_{HSI} image is enhanced to increase its contrast, similarly to grayscale images. In the final step, the improved I -channel, along with the H and S planes, is converted back to the RGB space. In this section, we compare the results of the proposed ICE-CCO algorithm with those produced by the CLAHE and MSA-ICE methods. To evaluate the effectiveness of each algorithm, we used six ($I_{c1} - I_{c6}$) representative images extracted from public datasets, and the results are presented in Table 8. According to Table 8, the images produced by the ICE-CCO approach have higher brightness and stronger color saturation, indicating better contrast compared to the images produced by the CLAHE and MSA-ICE methods. On the other hand, the CLAHE and MSA-ICE methods produce images with a darker perception. One of the significant differences between the images produced by the ICE-CCO and those produced by the CLAHE and MSA-ICE is the color saturation. The ICE-CCO algorithm produces images with clearer boundaries between objects with different brightness or color, while the CLAHE and MSA-ICE methods produce low-contrast areas that appear more homogeneous. Additionally, the images produced by the ICE-CCO algorithm contain more details that are only visible in its produced high-contrast images. In contrast, several essential structures of the image remain hidden in the images produced by the CLAHE and MSA-ICE methods. It's also important to note that the CLAHE method produces images with acceptable contrast. However, most of them look unnatural due to oversaturation of the colors as a consequence of a deficient way to distribute the pixels in the color planes. Overall, the proposed ICE-CCO algorithm outperforms the CLAHE and MSA-ICE methods in terms of contrast enhancement and preservation of the original image details. The images produced by the ICE-CCO algorithm have higher brightness, stronger color saturation, and clearer boundaries between objects with different brightness or color, resulting in a more natural and visually appealing image.

Table 9 presents a comparison of the performance of three different image enhancement methods, namely CLAHE, MSA-ICE, and ICE-CCO. The evaluation is based on six performance indexes, namely Mean squared error (*MSE*), Structural similarity index measurement (*SSIM*), Edge Preserve Index (*EPI*), Entropy (*E*), Relative Enhancement Contrast (*REC*), Range Redistribution (*RR*) and Visual Information Fidelity (*VIF*). In addition to the aforementioned indices, the Colorfulness (*C*) index is also incorporated.

The index *MSE* measures the similarity between the enhanced image and its reference, while *SSIM* measures the similarity between the improved image and the original. According to Table 9, the ICE-CCO algorithm performs

TABLE 7. Histogram comparison between ICE-CCO, CLAHE, and MSA-ICE.

better than the other two methods in terms of both MSE and SSIM values. This indicates that the ICE-CCO produces

images that are more similar to both the reference and the original images, respectively, with less distortion. The EPI

TABLE 8. Visual comparison between ICE-CCO, CLAHE and MSA-ICE.

ORIGINAL	CLAHE	MSA-ICE	ICE-CCO	
I_{C1}				
I_{C2}				
I_{C3}				
I_{C4}				
I_{C5}				
I_{C6}				

measures the preservation of edges in the enhanced image in comparison to the original image. The ICE-CCO method

outperforms the other two methods in terms of EPI, which means that it preserves the edges of the original image in

TABLE 9. Experimental comparison between CLAHE, MSA-ICE, and ICE-CCO with color images.

Image	Metric	CLAHE	MSA-ICE	ICE-CCO
I ₁	<i>SSIM</i>	0.7651	0.8854	0.9994
	<i>MSE</i>	8.87E+03	8.01E+03	0.0041
	<i>EPI</i>	0.9874	1.1247	0.9888
	<i>E</i>	5.7428	6.7421	7.3135
	<i>REC</i>	1.0094	1.1241	1.0912
	<i>RR</i>	38.2170	44.2781	86.3887
	<i>C</i>	0.2978	0.3341	0.3447
I ₂	<i>VIF</i>	1.1728	1.6845	1.9405
	<i>SSIM</i>	0.5832	0.7021	0.9982
	<i>MSE</i>	6.75E+03	6.17E+03	0.0124
	<i>EPI</i>	0.8941	0.9874	0.9944
	<i>E</i>	3.7024	4.8821	7.0275
	<i>REC</i>	0.8741	0.9441	1.0603
	<i>RR</i>	32.0147	38.1420	65.1640
I ₃	<i>C</i>	0.2417	0.3011	0.3651
	<i>VIF</i>	1.2490	1.4383	2.9105
	<i>SSIM</i>	0.7104	0.8421	0.9983
	<i>MSE</i>	7.93E+03	7.32E+03	0.0128
	<i>EPI</i>	0.8621	0.9421	0.9895
	<i>E</i>	3.1421	4.1014	6.8529
	<i>REC</i>	0.7721	0.8941	1.0777
I ₄	<i>RR</i>	30.8740	36.2140	58.1968
	<i>C</i>	0.2422	0.2987	0.0453
	<i>VIF</i>	1.1829	1.2966	1.7951
	<i>SSIM</i>	0.6931	0.8021	0.9984
	<i>MSE</i>	8.84E+03	7.89E+03	0.0109
	<i>EPI</i>	0.8654	0.9765	0.9976
	<i>E</i>	3.7892	4.5672	7.1957
I ₅	<i>REC</i>	0.8021	0.9023	1.0808
	<i>RR</i>	30.2385	37.9632	79.9972
	<i>C</i>	0.1892	0.2893	0.1504
	<i>VIF</i>	1.2678	1.5267	2.4386
	<i>SSIM</i>	0.8122	0.9032	0.9985
	<i>MSE</i>	8.58E+03	7.81E+03	0.0116
	<i>EPI</i>	0.8840	0.9902	0.9948
I ₆	<i>E</i>	3.6783	5.0393	7.6193
	<i>REC</i>	0.9054	1.0342	1.1293
	<i>RR</i>	29.9045	39.8701	98.2546
	<i>C</i>	0.2076	0.3678	0.0390
	<i>VIF</i>	1.3270	1.3891	1.4742
	<i>SSIM</i>	0.8122	0.9032	0.9977
	<i>MSE</i>	8.58E+03	7.81E+03	0.0157
	<i>EPI</i>	0.8840	0.9902	0.9870
	<i>E</i>	3.6783	5.0393	6.6304
	<i>REC</i>	0.9054	1.0342	1.0782
	<i>RR</i>	29.9045	39.8701	42.8217
	<i>C</i>	0.2076	0.3678	0.3721
	<i>VIF</i>	1.2521	1.4863	2.1012

the enhanced image better. However, the MSA-ICE method also performs well in terms of EPI. The Entropy (E) index assesses the information content and the number of details in

the enhanced image. The ICE-CCO method produces images with higher entropy values than the other two methods, indicating that it enhances contrast while preserving essential details. The RR measures the redistribution of pixel intensities in the enhanced image. The ICE-CCO method is better than the other two methods in terms of RR, indicating that it distributes the pixel intensities in the enhanced image better. Finally, the REC measures the contrast enhancement between the enhanced image and the original image. The proposed ICE-CCO method performs better in terms of REC values than the other two methods, indicating that it provides better contrast enhancement results. The VIF index was used to evaluate the visual quality of the images in terms of human perception. The results indicate that the ICE-CCO method produces images with the highest values of VIF, which means that these images have the best visual quality according to human perception. The MSA-ICE method comes in second place, with lower values than ICE-CCO. Conversely, the CLAHE method produces images with the worst visual quality, as it has the lowest values of VIF.

Overall, the ICE-CCO algorithm outperforms the CLAHE and MSA-ICE methods in terms of MSE, SSIM, EPI, Entropy (E), RR, REC and VIF. These results demonstrate that the ICE-CCO method is effective in enhancing the contrast of images while preserving important details and edges. In the experiment, several performance indexes were used to evaluate the effectiveness of the different contrast enhancement methods. While each index provides valuable information about the image quality, the Colorfulness (C) index stands out as the most descriptive in terms of color perception. The Colorfulness (C) index evaluates the color saturation of an image, indicating how vivid and intense the colors are. This index is particularly relevant when the enhancement of color images is the objective, as it provides valuable information about the perceived quality of the color in the image. From Table 9, it is evident that the proposed ICE-CCO method obtained the best Colorfulness (C) values compared to the other two methods. This fact indicates that the ICE-CCO algorithm produces images with more vivid and intense colors, which results in a better overall impression according to the human observer.

E. IMAGE NOISE REMOVAL TESTING

The proposed method has the particularity of improving the image quality in terms of contrast even in images that have been degraded by noise or other artifacts. Homomorphic filtering (HF) is a technique that improves the contrast of an image by separating the illumination and reflectance components of the image. In the presence of noise, the illumination component of an image can become uneven, resulting in poor contrast and visibility of the objects in the scene. To address this issue, HF applies a logarithmic transform to the image. The logarithmic transform enhances the low-intensity regions of the image. Therefore, the presence of noise and artifacts tend to be reduced.

TABLE 10. Image denoising metrics.

Metric	Ig1	Ig2	Ig3	Ig4	
ICE-CCO	PSNR	32.466	32.859	29.899	38.762
	SSIM	1.0000	1.0000	0.9999	0.9999
	MSE	0.6743	0.6823	0.6742	0.7021
	EPI	0.9770	0.9920	0.9932	0.9897
	RR	80.195	135.75	159.15	113.39
	REC	1.0222	1.0056	1.0341	1.0382
	E	6.2752	7.4568	7.3596	7.3329
	C	0.1890	0.0334	0.1132	0.0639
	VIF	1.2737	1.3175	1.5035	1.5420
ICE-CSOBHE	PSNR	22.381	22.083	22.192	21.807
	SSIM	0.8643	0.8893	0.9002	0.9088
	MSE	0.8932	0.8892	0.8111	0.9007
	EPI	0.9766	0.9920	0.9925	0.9886
	RR	79.682	133.70	165.69	120.15
	REC	1.0214	1.0027	1.0136	1.0284
	E	6.2729	7.4484	7.2836	7.3287
	C	0.1915	0.0335	0.1205	0.0660
	VIF	1.0701	1.0093	1.0408	1.1289

To evaluate the performance of the approach in the presence of noise, a new experiment is conducted. The experiment aims to analyze how well the proposed method performs in improving the contrast of images that are contaminated with Gaussian noise. For this process, a set of representative images with bad contrast and distortions is selected. The selected images are then artificially contaminated with Gaussian noise. The amount and intensity of the noise are controlled to ensure that the images have a variety of levels of noise. Finally, a method is used to improve the contrast of the contaminated images.

In this experiment the results of the proposed approach are compared with those produced by the CSOBHE algorithm [51] which is a state-of-the-art method for image contrast enhancement with capacities to reduce the noise effect. The CSOBHE algorithm is a contrast-limited adaptive histogram equalization (CLAHE) based algorithm that applies a nonlinear mapping function on the histogram of the image in order to equalize the contrast of the image. The algorithm employs an optimized thresholding function and a constrained optimization technique based on the Cuckoo Search algorithm [52] to enhance the contrast of the image while reducing the effect of noise.

Table 10 shows the images used in the experiment to evaluate the performance of the proposed method in improving the contrast of contaminated images. The table consists of three columns. The first column presents the original image. The second column shows the corresponding contaminated versions of the original images, where each image has been artificially contaminated with Gaussian noise. The third column displays the resulting images after processing with the proposed method. According to the results shown in Table 10, the proposed method is effective in improving the contrast of the contaminated images. The enhanced images show improved image quality with small effects of

saturation. The method also preserves the edges in the images while highlighting hidden details in low contrast images and reducing the noise structures. Despite the interesting results, the proposed approach has a limitation. When the image is severely damaged by noise, the method cannot restore the original colors accurately. This is a common issue with image processing methods that attempt to enhance the image quality of contaminated images. Therefore, it is important to consider the level of noise and damage in the original images when selecting an appropriate image enhancement technique. On the other hand, when comparing the results of the CSOBHE algorithm with the proposed approach, it becomes evident that the CSOBHE algorithm presents images with poor contrast. The colors in the images have been distorted as a result of the presence of noise, leading to an overall degradation of image quality. One notable drawback of the CSOBHE algorithm is its limited ability to simultaneously improve contrast and reduce the presence of noise. As a consequence, several artifacts remain present in the images, hindering the visual interpretation of the content. The borders and other fine structures in the images are particularly affected, as the algorithm fails to effectively enhance the contrast while preserving the details and boundaries. The inability of the CSOBHE algorithm to eliminate artifacts and preserve the natural appearance of the images is a significant limitation. The distorted colors and the presence of artifacts can adversely impact the visual perception and interpretation of the images. This limitation hinders the algorithm's suitability for applications where accurate image analysis and faithful representation of the original content are essential. In contrast, the proposed approach demonstrates its capability to improve both contrast and reduce noise, resulting in enhanced images with improved visual quality. The proposed method effectively highlights hidden details in low contrast images while significantly reducing the noise structures. The edges and other important structures are preserved, maintaining the overall integrity of the image. The clear disparity between the results obtained from the CSOBHE algorithm and the proposed approach emphasizes the superiority of the latter in terms of contrast enhancement and noise reduction. The proposed approach successfully addresses the limitations observed in the CSOBHE algorithm, providing visually appealing images with improved contrast, reduced noise, and enhanced image quality.

Table 11 presents the performance indexes for the resulting enhanced images after applying both methods to improve the contrast of images contaminated with noise. The evaluation is based on six performance indexes: Mean Squared Error (*MSE*), Structural Similarity Index Measurement (*SSIM*), Edge Preserve Index (*EPI*), Entropy (*E*), Relative Enhancement Contrast (*REC*), Range Redistribution (*RR*), The Peak Signal-to-Noise Ratio (*PSNR*), the Colorfulness (*C*) index and the Visual Information Fidelity (*VIF*). In general terms, the performance indexes obtained by the proposed approach are better than the produced by the CSOBHE algorithm. From all indexes, the *PSNR* metric is an important

TABLE 11. Visual results from image denoising.

image	ORIGINAL	NOISY	ICE-CSOBHE	ICE-CCO
Ig1				
Ig2				
Ig3				
Ig4				

measure of image preservation and quality, especially when images contain noise. It measures the ratio between the maximum possible power of a signal and the power of corrupting noise that affects the fidelity of its representation. The higher the PSNR value, the smaller the amount of noise in the image. According to the PSNR values in Table 11, the proposed method significantly reduces the noise level in the enhanced images compared to the CSOBHE method. This indicates that the proposed method is more effective in improving the contrast of images contaminated with noise while preserving their image quality than the CSOBHE method. Another important metric is the VIF index, which indicates the quality of the image in terms of a human observer. According to its values in Table 11, the proposed approach obtains the highest values, indicating that the proposed method is able to produce images with more quality in terms of a human observer than the CSOBHE algorithm.

V. CONCLUSION

Homomorphic filtering is an image processing technique that allows to separate the illumination and reflectance components of an image. The main advantage of homomorphic filtering over linear filtering is its ability to enhance the low-frequency components of an image while suppressing the high-frequency components, without affecting the edges

or sharp features of the image. The parameters of the homomorphic filter affect the enhancement quality of the output image. Finding the optimal values for these parameters can be difficult because they depend on various factors such as the illumination conditions and the noise level. Determining the correct parameters for a homomorphic filter often involves a trial-and-error process, where different parameter values are tested until the desired output is achieved. This can be time-consuming and requires a good understanding of the underlying principles of homomorphic filtering. In this paper, a metaheuristic method known as cluster-chaotic optimization method is used to identify the optimal values of the filter parameters by evaluating an objective function, which represents the quality of the output image. The algorithm uses chaotic sequences to effectively explore the search space and avoid getting stuck in local optima, which leads to a faster convergence to the global optimum. This is particularly advantageous for complex optimization problems with a large search space, where other optimization methods may require a long computation time to find the optimal solution.

Our proposed approach for image enhancement has undergone rigorous testing to ensure its effectiveness. To test the approach, we used a set of representative images extracted from different databases [48], [49]. To assess the performance of our method, we compared its results with those produced

by other popular and state-of-the-art techniques. This comparison was conducted using several performance indexes that assess the visual quality of the enhanced images. The results of our testing clearly demonstrate that our method produces competitive results in terms of quality, stability, and accuracy. Our approach outperforms other techniques in many cases, producing enhanced images that are more visually pleasing and accurate than those produced by other methods. The proposed method has been evaluated for its ability to improve image contrast under noisy conditions. The outcomes showed that our approach was capable of enhancing contrast adequately while introducing minimal color distortion. This indicates that our technique is effective in improving image contrast even in situations where noise is present, and it maintains a natural and balanced color representation.

Some directions that deserve future work include the use of multi-objective optimization to consider different elements for segmentation and the exploration of the advantages of enhancing the results by using a locally enlarged image method.

REFERENCES

- [1] T. D. Pham, "Kriging-weighted Laplacian kernels for grayscale image sharpening," *IEEE Access*, vol. 10, pp. 57094–57106, 2022, doi: [10.1109/ACCESS.2022.3178607](https://doi.org/10.1109/ACCESS.2022.3178607).
- [2] T. Ma, L. Li, S. Ji, X. Wang, Y. Tian, A. Al-Dhelaan, and M. Al-Rodhaan, "Optimized Laplacian image sharpening algorithm based on graphic processing unit," *Phys. A, Stat. Mech. Appl.*, vol. 416, pp. 400–410, Dec. 2014, doi: [10.1016/J.PHYSA.2014.09.026](https://doi.org/10.1016/J.PHYSA.2014.09.026).
- [3] F. Zhang, W. Xie, G. Ma, and Q. Qin, "High dynamic range compression and detail enhancement of infrared images in the gradient domain," *Infr. Phys. Technol.*, vol. 67, pp. 441–454, Nov. 2014, doi: [10.1016/J.INFRARED.2014.09.003](https://doi.org/10.1016/J.INFRARED.2014.09.003).
- [4] S. C. F. Lin, C. Y. Wong, M. A. Rahman, G. Jiang, S. Liu, N. Kwok, H. Shi, Y.-H. Yu, and T. Wu, "Image enhancement using the averaging histogram equalization (AVHEQ) approach for contrast improvement and brightness preservation," *Comput. Electr. Eng.*, vol. 46, pp. 356–370, Aug. 2015, doi: [10.1016/J.COMPELECEENG.2015.06.001](https://doi.org/10.1016/J.COMPELECEENG.2015.06.001).
- [5] P. Yugander, C. H. Tejaswini, J. Meenakshi, K. S. Kumar, B. V. N. S. Varma, and M. Jagannath, "MR image enhancement using adaptive weighted mean filtering and homomorphic filtering," *Proc. Comput. Sci.*, vol. 167, pp. 677–685, Jan. 2020, doi: [10.1016/j.procs.2020.03.334](https://doi.org/10.1016/j.procs.2020.03.334).
- [6] R. Al Sobbahi and J. Tekli, "Low-light homomorphic filtering network for integrating image enhancement and classification," *Signal Process., Image Commun.*, vol. 100, Jan. 2022, Art. no. 116527, doi: [10.1016/j.image.2021.116527](https://doi.org/10.1016/j.image.2021.116527).
- [7] W. Zhang, Y. Wang, and C. Li, "Underwater image enhancement by attenuated color channel correction and detail preserved contrast enhancement," *IEEE J. Ocean. Eng.*, vol. 47, no. 3, pp. 718–735, Jul. 2022.
- [8] A. Draa and A. Bouaziz, "An artificial bee colony algorithm for image contrast enhancement," *Swarm Evol. Comput.*, vol. 16, pp. 69–84, Jun. 2014, doi: [10.1016/j.swevo.2014.01.003](https://doi.org/10.1016/j.swevo.2014.01.003).
- [9] U. Kuran and E. C. Kuran, "Parameter selection for CLAHE using multi-objective cuckoo search algorithm for image contrast enhancement," *Intell. Syst. Appl.*, vol. 12, Nov. 2021, Art. no. 200051, doi: [10.1016/J.ISWA.2021.200051](https://doi.org/10.1016/J.ISWA.2021.200051).
- [10] M. Mozumi, R. Nagaoka, and H. Hasegawa, "Improving image contrast and accuracy in velocity estimation by convolution filters for intracardiac blood flow imaging," *Ultrasonics*, vol. 120, Mar. 2022, Art. no. 106650, doi: [10.1016/j.ultras.2021.106650](https://doi.org/10.1016/j.ultras.2021.106650).
- [11] I. S. Isa, S. N. Sulaiman, M. Mustapha, and N. K. A. Karim, "Automatic contrast enhancement of brain MR images using average intensity replacement based on adaptive histogram equalization (AIR-AHE)," *Biocybernetics Biomed. Eng.*, vol. 37, no. 1, pp. 24–34, 2017, doi: [10.1016/J.BBE.2016.12.003](https://doi.org/10.1016/J.BBE.2016.12.003).
- [12] N. Singh, L. Kaur, and K. Singh, "Histogram equalization techniques for enhancement of low radiance retinal images for early detection of diabetic retinopathy," *Eng. Sci. Technol., Int. J.*, vol. 22, no. 3, pp. 736–745, Jun. 2019, doi: [10.1016/j.jestch.2019.01.014](https://doi.org/10.1016/j.jestch.2019.01.014).
- [13] W. Zhang, P. Zhuang, H. Sun, G. Li, S. Kwong, and C. Li, "Underwater image enhancement via minimal color loss and locally adaptive contrast enhancement," *IEEE Trans. Image Process.*, vol. 31, pp. 3997–4010, 2022.
- [14] W. Zhang, S. Jin, P. Zhuang, Z. Liang, and C. Li, "Underwater image enhancement via piecewise color correction and dual prior optimized contrast enhancement," *IEEE Signal Process. Lett.*, vol. 30, pp. 229–233, 2023.
- [15] A. Cozzi, V. Magni, M. Zanardo, S. Schiaffino, and F. Sardanelli, "Contrast-enhanced mammography: A systematic review and meta-analysis of diagnostic performance," *Radiology*, vol. 302, no. 3, pp. 568–581, Mar. 2022.
- [16] W. Ma, N. Li, H. Zhu, L. Jiao, X. Tang, Y. Guo, and B. Hou, "Feature split-merge-enhancement network for remote sensing object detection," *IEEE Trans. Geosci. Remote Sens.*, vol. 60, 2022, Art. no. 5616217.
- [17] W. Zhi-She, Y. Feng-Bao, P. Zhi-Hao, C. Lei, and J. Lie, "Multi-sensor image enhanced fusion algorithm based on NSST and top-hat transformation," *Optik*, vol. 126, no. 23, pp. 4184–4190, Dec. 2015, doi: [10.1016/J.IJOLEO.2015.08.118](https://doi.org/10.1016/J.IJOLEO.2015.08.118).
- [18] J. C. M. Román, R. Escobar, F. Martínez, J. L. V. Noguera, H. Legal-Ayala, and D. P. Pinto-Roa, "Medical image enhancement with brightness and detail preserving using multiscale top-hat transform by reconstruction," *Electron. Notes Theor. Comput. Sci.*, vol. 349, pp. 69–80, Jun. 2020, doi: [10.1016/J.ENTCS.2020.02.013](https://doi.org/10.1016/J.ENTCS.2020.02.013).
- [19] *Homomorphic Filtering—Part 1 >> Steve on Image Processing With MATLAB—MATLAB & Simulink*. Accessed: Jan. 30, 2022. [Online]. Available: <https://blogs.mathworks.com/steve/2013/06/25/homomorphic-filtering-part-1/>
- [20] *Homomorphic Filtering—Part 2 >> Steve on Image Processing With MATLAB—MATLAB & Simulink*. Accessed: Jan. 30, 2022. [Online]. Available: https://blogs.mathworks.com/steve/2013/07/10/homomorphic-filtering-part-2/?doing_wp_cron=1643666709.9516789913177490234375
- [21] E. Daniel, "Optimum wavelet-based homomorphic medical image fusion using hybrid genetic-grey wolf optimization algorithm," *IEEE Sensors J.*, vol. 18, no. 16, pp. 6804–6811, Aug. 2018, doi: [10.1109/JSEN.2018.2822712](https://doi.org/10.1109/JSEN.2018.2822712).
- [22] L. Zhang, J. Xia, X. Ying, Y. He, W. Mueller-Wittig, and H.-S. Seah, "Efficient and robust 3D line drawings using difference-of-Gaussian," *Graph. Models.*, vol. 74, no. 4, pp. 87–98, Jul. 2012, doi: [10.1016/J.GMOD.2012.03.006](https://doi.org/10.1016/J.GMOD.2012.03.006).
- [23] P. Birch, B. Mitra, N. M. Bangalore, S. Rehman, R. Young, and C. Chatwin, "Approximate bandpass and frequency response models of the difference of Gaussian filter," *Opt. Commun.*, vol. 283, no. 24, pp. 4942–4948, Dec. 2010, doi: [10.1016/J.OPTCOM.2010.07.047](https://doi.org/10.1016/J.OPTCOM.2010.07.047).
- [24] X. S. Yang, *Nature-Inspired Optimization Algorithms*. London, U.K.: Academic, 2020.
- [25] T. Dokeroğlu, E. Sevinc, T. Kucukyilmaz, and A. Cosar, "A survey on new generation metaheuristic algorithms," *Comput. Ind. Eng.*, vol. 137, Nov. 2019, Art. no. 106040, doi: [10.1016/j.cie.2019.106040](https://doi.org/10.1016/j.cie.2019.106040).
- [26] Q. Lu, Y. Ren, H. Jin, L. Meng, L. Li, C. Zhang, and J. W. Sutherland, "A hybrid metaheuristic algorithm for a profit-oriented and energy-efficient disassembly sequencing problem," *Robot. Comput.-Integr. Manuf.*, vol. 61, Feb. 2020, Art. no. 101828, doi: [10.1016/j.rcim.2019.101828](https://doi.org/10.1016/j.rcim.2019.101828).
- [27] J. Kennedy and R. Eberhart, "Particle swarm optimization," in *Proc. IEEE ICNN*, vol. 4, Nov./Dec. 1995, pp. 1942–1948, doi: [10.1109/ICNN.1995.488968](https://doi.org/10.1109/ICNN.1995.488968).
- [28] M. Jafari, E. Salajegheh, and J. Salajegheh, "Optimal design of truss structures using a hybrid method based on particle swarm optimizer and cultural algorithm," *Structures*, vol. 32, pp. 391–405, Aug. 2021, doi: [10.1016/J.ISTRUC.2021.03.017](https://doi.org/10.1016/J.ISTRUC.2021.03.017).
- [29] S. Kumar, B. Sharma, V. K. Sharma, H. Sharma, and J. C. Bansal, "Plant leaf disease identification using exponential spider monkey optimization," *Sustain. Computing: Informat. Syst.*, vol. 28, Dec. 2018, Art. no. 100283, doi: [10.1016/J.SUSCOM.2018.10.004](https://doi.org/10.1016/J.SUSCOM.2018.10.004).
- [30] S. Mirjalili, S. M. Mirjalili, and A. Lewis, "Grey wolf optimizer," *Adv. Eng. Softw.*, vol. 69, pp. 46–61, Mar. 2014, doi: [10.1016/j.advengsoft.2013.12.007](https://doi.org/10.1016/j.advengsoft.2013.12.007).

- [31] A. S. Joshi, O. Kulkarni, G. M. Kakandikar, and V. M. Nandedkar, "Cuckoo search optimization—A review," *Mater. Today, Proc.*, vol. 4, no. 8, pp. 7262–7269, 2017, doi: [10.1016/J.MATPR.2017.07.055](https://doi.org/10.1016/J.MATPR.2017.07.055).
- [32] J. Cheng, L. Wang, and Y. Xiong, "Ensemble of cuckoo search variants," *Comput. Ind. Eng.*, vol. 135, pp. 299–313, Sep. 2019, doi: [10.1016/J.CIE.2019.06.015](https://doi.org/10.1016/J.CIE.2019.06.015).
- [33] P. Wu, H. Wang, B. Li, W. Fu, J. Ren, and Q. He, "Disassembly sequence planning and application using simplified discrete gravitational search algorithm for equipment maintenance in hydropower station," *Exp. Syst. Appl.*, vol. 208, Dec. 2022, Art. no. 118046, doi: [10.1016/J.ESWA.2022.118046](https://doi.org/10.1016/J.ESWA.2022.118046).
- [34] H. R. Patel and V. A. Shah, "Comparative analysis between two fuzzy variants of harmonic search algorithm: Fuzzy fault tolerant control application," *IFAC-PapersOnLine*, vol. 55, no. 7, pp. 507–512, 2022, doi: [10.1016/J.IFACOL.2022.07.494](https://doi.org/10.1016/J.IFACOL.2022.07.494).
- [35] R. M. Gray, *Entropy and Information Theory*. Heidelberg, Germany: Springer, 2011.
- [36] S. Hinojosa, K. G. Dhal, M. A. Elaziz, D. Oliva, and E. Cuevas, "Entropy-based imagery segmentation for breast histology using the stochastic fractal search," *Neurocomputing*, vol. 321, pp. 201–215, Dec. 2018, doi: [10.1016/J.NEUCOM.2018.09.034](https://doi.org/10.1016/J.NEUCOM.2018.09.034).
- [37] J. Gálvez, E. Cuevas, H. Becerra, and O. Avalos, "A hybrid optimization approach based on clustering and chaotic sequences," *Int. J. Mach. Learn. Cybern.*, vol. 11, no. 2, pp. 359–401, Feb. 2020, doi: [10.1007/s13042-019-00979-6](https://doi.org/10.1007/s13042-019-00979-6).
- [38] Y. Li, M. Otsubo, R. Kuwano, and S. Nadimi, "Quantitative evaluation of surface roughness for granular materials using Gaussian filter method," *Powder Technol.*, vol. 388, pp. 251–260, Aug. 2021, doi: [10.1016/j.powtec.2021.04.068](https://doi.org/10.1016/j.powtec.2021.04.068).
- [39] L. D. S. Coelho, J. G. Sauer, and M. Rudek, "Differential evolution optimization combined with chaotic sequences for image contrast enhancement," *Chaos, Solitons Fractals*, vol. 42, no. 1, pp. 522–529, Oct. 2009.
- [40] C. Munteanu and A. Rosa, "Gray-scale image enhancement as an automatic process driven by evolution," *IEEE Trans. Syst., Man Cybern., B Cybernetics*, vol. 34, no. 2, pp. 1292–1298, Apr. 2004, doi: [10.1109/TSMCB.2003.818533](https://doi.org/10.1109/TSMCB.2003.818533).
- [41] S. B. Carlos, *Física del Caos en la Predicción Meteorológica*. Madrid, Spain: Agencia Estatal de Meteorología, 2018, pp. 49–65.
- [42] B. Kim, K. H. Ryu, and S. Heo, "Mean squared error criterion for model-based design of experiments with subset selection," *Comput. Chem. Eng.*, vol. 159, Mar. 2022, Art. no. 107667, doi: [10.1016/j.compchemeng.2022.107667](https://doi.org/10.1016/j.compchemeng.2022.107667).
- [43] A. Hore and D. Ziou, "Image quality metrics: PSNR vs. SSIM," in *Proc. 20th Int. Conf. Pattern Recognit.*, Aug. 2010, pp. 2366–2369, doi: [10.1109/ICPR.2010.579](https://doi.org/10.1109/ICPR.2010.579).
- [44] R. Nie, M. He, J. Cao, D. Zhou, and Z. Liang, "Pulse coupled neural network based MRI image enhancement using classical visual receptive field for smarter mobile healthcare," *J. Ambient Intell. Humanized Comput.*, vol. 10, no. 10, pp. 4059–4070, Oct. 2019.
- [45] C. Zhao, Z. Wang, H. Li, X. Wu, S. Qiao, and J. Sun, "A new approach for medical image enhancement based on luminance-level modulation and gradient modulation," *Biomed. Signal Process. Control*, vol. 48, pp. 189–196, Feb. 2019.
- [46] Z. Chen, B. R. Abidi, D. L. Page, and M. A. Abidi, "Gray-level grouping (GLG): an automatic method for optimized image contrast enhancement—part I: the basic method," *IEEE Trans. Image Process.*, vol. 15, no. 8, pp. 2290–2302, Aug. 2006.
- [47] *Messier Catalog*, NASA, Washington, DC, USA, 2022. [Online]. Available: <https://www.nasa.gov/content/goddard/hubble-s-messier-catalog>
- [48] N. Ponomarenko, L. Jin, O. Ieremeiev, V. Lukin, K. Egiazarian, J. Astola, B. Vozel, K. Chehdi, M. Carli, F. Battisti, and C.-C. J. Kuo, "Image database TID2013: Peculiarities, results and perspectives," *Signal Process., Image Commun.*, vol. 30, pp. 57–77, Jan. 2015, doi: [10.1016/j.image.2014.10.009](https://doi.org/10.1016/j.image.2014.10.009).
- [49] A. G. Weber. (2018). *The USC-SIPI Image Database: Version 6*. [Online]. Available: <http://netpbm.sourceforge.net/>
- [50] D. Hasler and S. E. Suesstrunk, "Measuring colorfulness in natural images," in *Proc. SPIE*, 2003, pp. 87–95.
- [51] N. Thakur, N. U. Khan, and S. Datt Sharma, "Cuckoo search optimized histogram equalization for low contrast image enhancement," in *Proc. 7th Int. Conf. Parallel, Distrib. Grid Comput. (PDGC)*, Nov. 2022, pp. 727–732.
- [52] X. S. Yang and S. Deb, "Cuckoo search via Lévy flights," in *Proc. World Congr. Nature Biologically Inspired Computing (NabIC)*, 2009, pp. 210–214.



ÁNGEL CHAVARÍN received the bachelor's degree in communications and electronics engineering and the Master of Science degree in electronics and computer engineering from the University of Guadalajara (UDG), where he is currently pursuing the Ph.D. degree in electronics and computer science with the University Center of Exact Sciences and Engineering (CUCEI). His research interests include artificial vision and neural networks and working on different projects to develop science.



ERIK CUEVAS received the B.S. degree (Hons.) in electronics and communications engineering from the University of Guadalajara, Mexico, in 1995, the M.Sc. degree in industrial electronics from ITESO, Mexico, in 2000, and the Ph.D. degree from Freie Universität Berlin, Germany, in 2006. Since 2006, he has been with the University of Guadalajara, where he is currently a full-time Professor with the Department of Computer Science. Since 2008, he has been a member of the Mexican National Research System (SNI III). His current research interests include metaheuristics and computer vision. He serves as an Associate Editor for *Artificial Intelligence Review*, *Expert Systems With Applications*, *ISA Transactions*, and *Applied Soft Computing*.



OMAR AVALOS received the Ph.D. degree in computer science and electronics from the Universidad de Guadalajara. He is currently working as a Professor with the Department of Computer Science, Universidad de Guadalajara. His research interests include metaheuristic and evolutionary computation for image processing, system identification, and energy applications.



JORGE GÁLVEZ received the B.S. degree in informatics, in 2011, the M.Sc. degree in electronics and computing, in 2015, and the Ph.D. degree in electronics and computer science from the Universidad de Guadalajara, in 2019. Since 2019, he has been a member of the Mexican National Research System (SNI I). He is currently working as a Professor with the Department of Computer Science, Universidad de Guadalajara. His research interests include the design and applications of metaheuristic algorithms, machine learning, complex systems, and robotics.



MARCO PÉREZ-CISNEROS received the B.S. degree (Hons.) in electronics and communications engineering from the University of Guadalajara, Mexico, in 1995, the M.Sc. degree in industrial electronics from ITESO University, Mexico, in 2000, and the Ph.D. degree from the University of Manchester Institute of Science and Technology, UMIST, Manchester, U.K., in 2004. He was a Research Consultant on robotic manipulators at TQ Ltd., U.K., in 2003, and since 2005, he has been with the University of Guadalajara, where he is currently a Professor and the Head of the Department of Computer Science. He has been a member of the Mexican National Research System (SNI), since 2007. His current research interests include robotics and computer vision, especially visual servoing and humanoid walking control.